ELSEVIER

Polymer 41 (2000) 1269–1276

polymer

Inverse microemulsion polymerization of MADQUAT initiated with sodium metabisulfite

A. Sáenz de Buruaga[1], J.C. de la Cal, J.M. Asua*

Grupo de Ingeniería Química, Departamento de Química Aplicada, Facultad de Ciencias Químicas, Universidad del País Vasco, Apdo 1072, 20080 San Sebastián, Spain

Received 9 March 1999; received in revised form 19 April 1999; accepted 23 April 1999

Abstract

The kinetics of the inverse microemulsion polymerization of MADQUAT initiated with sodium metabisulfite in both batch and semi-continuous reactors was studied using reaction calorimetry. It was found that the metabisulfite was able to initiate the polymerization at low temperature (20°C) and that in batch reactor the polymerization stopped well before the complete conversion of the monomer due to complete consumption of the initiator, which disappeared according to first-order kinetics. High conversions were reached in short periods of time when the initiator was continuously fed during the process. In the semi-continuous process, the transport of metabisulfite from the droplets of the initiator solution to the particles seemed to be diffusionally limited and was accelerated by the availability of the emulsifier. The polymerization rate showed a complex evolution during the process owing to the interplay between transport phenomena, polymerization and initiation rates, and nucleation rate.

Keywords: Inverse microemulsion polymerization; MADQUAT; Redox initiation

1. Introduction

Microemulsions are thermodynamically stable dispersions produced by using surfactants able to reduce the interfacial energy to values close to zero. Both oil-in-water (direct) and water-in-oil (inverse) microemulsions can be produced but higher volumes of the disperse phase can be attained using inverse microemulsions [1]. The polymerization of inverse microemulsions of aqueous solutions of water-soluble monomers is an attractive way to produce high molecular-weight water-soluble polymers that can be used advantageously as flocculants in waste-water treatment and enhanced oil recovery [2–4]. Sáenz de Buruaga et al. [5] studied the kinetics of the inverse microemulsion polymerization of 2-methacryloyl oxyethyl trimethyl ammonium chloride (MADQUAT) initiated by UV light in the presence of azobisisobutyronitrile (AIBN). It was found that high molecular-weight water-soluble polymers could be obtained in short process times in a batch reactor. They discussed the implementation of the process in large-scale tank reactors and concluded that this may be difficult because of the high heat-generation rate, the low heat-removal capacity of these reactors and the problems associated with carrying out photoinitiated polymerization in a large reactor. Tubular reactors seemed to be the natural alternative as they have a large heat-transfer-area to reactor-volume ratio and the thermodynamically stable microemulsions can be easily pumped without phase separation or coagulation. The implementation of a photo-initiated process in a tubular reactor under conditions similar to those used in the batch reactor would require the UV irradiation of the whole tube, but this will deteriorate the heat transfer characteristics of the system. The alternative of irradiating only in some points of the reactor was checked and it was found that polymerization stopped shortly after the cessation of the irradiation [5].

In an attempt to find processes that were easier to implement, Sáenz de Buruaga [6] studied different redox initiation systems and reported that polymerization of MADQUAT occurred at quite a fast reaction rate in the presence of sodium metabisulfite. The ability of the metabisulfites to initiate the polymerization of different monomers have been reported [7–9]. Mukherjee et al. [7] found that the metabisulfite and bisulfite were able to initiate the aqueous phase polymerization of methyl methacrylate, ethyl methacrylate and methacrylic acid, as well as the polymerization of styrene, although a long inhibition period was

* Corresponding author.
E-mail address: gppasgoj@sq.ehu.es (J.M. Asua)
[1] Current address: C.A.F. (Div. 4), c/J.M. Iturrioz 26, 20200-Beasain, Spain.

0032-3861/00/$ - see front matter
PII: S0032-3861(99)00300-6

Table 1
Recipes used in the batch polymerizations at $T = 20°C$

Run	Aqueous phase (g)	Emulsifier (g)	Cyclohexane (g)	$S_2O_5Na_2$ (g)	X_{tf}	d_p (nm)	N_p (particles)
1	392.30	150.93	617.77	0.0275	0.66	99	3.81×10^{17}
2	392.30	150.93	617.77	0.0147	0.47	116	1.76×10^{17}

observed in this case. In contrast, metabisulfite and bisulfite were unable to initiate the polymerization of acrylonitrile, methyl acrylate and vinyl acetate. Mukherjee et al. [7] proposed the following reaction mechanism involving bisulfite ions that result from the metabisulfite [10]:

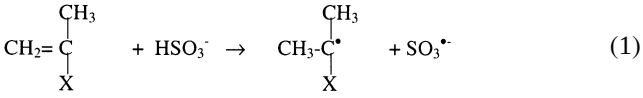

(1)

According to Mukherjee et al. [7], the activity of the $CH_3{-}C^{\cdot}X{-}CH_3$ radical is sterically reduced, and the low reactivity of this radical is what makes the initiation of methacrylates by the metabisulfite possible. Other vinylic monomers ($CH_2{=}CHX$) also react with the metabisulfite, but the radicals formed ($C^{\cdot}H_2{-}CH_2X$ or $CH_3{-}C^{\cdot}HX$) terminate quickly with the $SO_3^{\cdot-}$ radical. Murkherjee et al. [7] justified the low reactivity of styrene in terms of its low water solubility.

MADQUAT has a methacrylic group that may react with HSO_3^- through a reaction scheme similar to that presented in Eq. (1), namely, forming an active radical ($SO_3^{\cdot-}$) and another less reactive ($CH_3{-}C^{\cdot}X{-}CH_3$). This possibility is particularly interesting in the inverse microemulsion polymerization of MADQUAT because both the monomer and the metabisulfite are dispersed in small droplets [5] (10–30 nm in diameter) where they would terminate quickly if both of them were reactive.

In this work, the kinetics of the inverse microemulsion polymerization of MADQUAT initiated by sodium metabisulfite is investigated. The effect of the initiator concentration, the emulsifier concentration, the amount of aqueous phase and the amount of disperse phase on the polymerization rate, monomer conversion, particle diameter and number of polymer particles is studied.

2. Experimental

Commercially available MADQUAT was supplied by Elf Atochem as a 75% w/w aqueous solution. The emulsifier system was a blend of sorbitan sesquioleate (Arlacel 83, ICI Surfactants) and Sorbitan monooleate with 20 ethylene oxide groups (Tween 80, ICI Surfactants). $Na_2S_2O_5$ (purity 96%, Panreac) was used as the initiator. All these materials were used as supplied. Deionized water and commercial cyclohexane were used after filtration. The aqueous phase was prepared by diluting two parts (in weight) of the 75% aqueous solution of MADQUAT with one part of water giving a 50% aqueous solution of MADQUAT. The oil phase was prepared by dissolving the emulsifiers in the appropriate amount of cyclohexane. The inverse microemulsion was formed by mixing both phases under mechanical agitation and sonicating the mixture for 12 min at room temperature using a Branson Sonifier 450 (intensity: 7, duty cycle: 80%). A transparent and stable microemulsion was obtained. The conductivity of the microemulsion was close to that of cyclohexane showing that the microemulsion had a globular structure, which was formed by micelles swollen with the aqueous phase.

Polymerizations were carried out at 20°C in a Mettler RC1 calorimeter reactor. Agitation was provided by an anchor stirrer (300 rpm). Oxygen was removed from the reactor by purging with high purity (<2 ppm of oxygen) nitrogen (5.4 cm^3/s for 1 h). The system is very sensitive to the presence of oxygen and samples could not be collected without affecting the reaction. Collecting data is not necessary to obtain the evolution of the monomer conversion as this can be estimated from the calorimetric measurements. The heat balance of the reaction medium is:

$$\left(\sum m_j C_{pj}\right)\frac{dT}{dt} = Q_g - Q_h - Q_f + Q_s + Q_c - Q_l \qquad (2)$$

where the left-hand side term represents the heat accumulated in the reactor, Q_g is the heat generation rate due to the polymerization, Q_h the heat flux across the reactor wall, Q_f the heat due to the feeds, Q_s and Q_c the heating due to stirring and the calibration heater, respectively, and Q_l the heat loss to the surroundings. The polymerization heat can be calculated from the other terms, if these can be

Table 2
Recipes used in the semi-continuous polymerizations at $T = 20°C$

Run	Aqueous phase (g)	Emulsifier (g)	Cyclohexane (g)	$S_2O_5Na_2$ feed rate (g/min)	[Monomer] ($mol/l_{microem.}$)	X_{tf}	d_p (nm)	N_p (particles)
3	392.30	150.93	617.77	0.000582	0.728	0.98	107	4.0×10^{17}
4	392.30	150.93	617.77	0.000331	0.728	0.99	116	3.1×10^{17}
5	325.08	150.93	684.99	0.000331	0.593	0.98	111	3.0×10^{17}
6	174.15	150.93	835.92	0.000331	0.305	0.96	90	2.9×10^{17}
7	325.08	127.71	708.08	0.000331	0.589	0.98	121	2.3×10^{17}

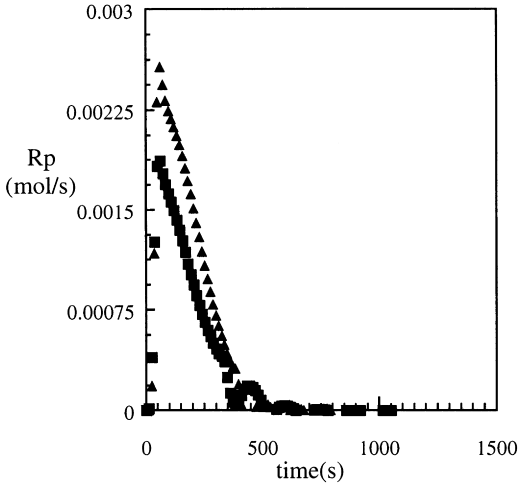

Fig. 1. Time evolution of the polymerization rate in the batch experiments: (▲) run 1; (■) run 2.

determined with sufficient accuracy, this being the essence of the reaction calorimetry. The equipment used allows for an accurate estimation of all terms in Eq. (2) [11–13]. The polymerization rate, R_p, is calculated as follows:

$$R_p = \frac{Q_g}{\int_0^{tf} Q_g \, dt} x_{tf} M_0 \quad (3)$$

where x_{tf} is the monomer conversion at the end of the reaction (which is measured by gas chromatography using butyl acrylate as an internal standard [5]) and M_0 the amount of monomer in the initial charge. The evolution of the conversion is calculated as

$$x = \frac{\int_0^t Q_g \, dt}{\int_0^{tf} Q_g \, dt} x_{tf}. \quad (4)$$

Both batch and semicontinuous polymerizations were carried out using the recipes given in Tables 1 and 2. In the batch processes, the inverse microemulsion was charged into the reactor, purged with nitrogen, brought to the reaction temperature and the polymerization was initiated by injecting an aqueous solution of $Na_2S_2O_5$. The polymerizations started without noticeable inhibition. In the semicontinuous reactions, the reactor was charged with the inverse microemulsion, purged with nitrogen, brought to the reaction temperature and at $t = 0$ a continuous feed of an aqueous solution of $Na_2S_2O_5$ was started. The polymerizations also started without inhibition.

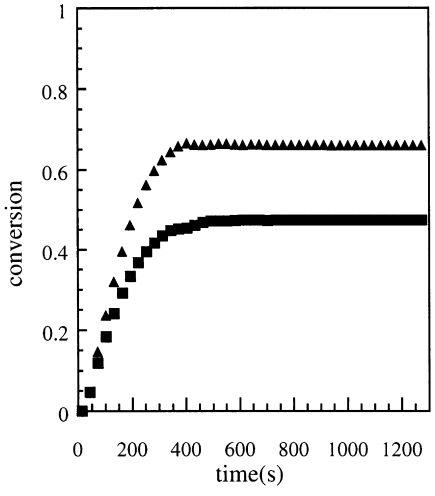

Fig. 2. Time evolution of the monomer conversion in the batch experiments: (▲) run 1; (■) run 2.

The particle size of the final latexes was determined by dynamic light scattering (DLS) using a Malvern 4700 apparatus at an angle of 90° and with an incident wavelength of 514.5 nm. The latex was diluted to 5% in volume with pure cyclohexane [5]. The number of particles was calculated from the values of the particle size and the monomer conversion assuming that all the polymer was in the particles and that water and monomer partitioning according the thermodynamic equilibrium. The partition coefficients were $k_M = k_W = 0.7$ [14].

3. Results and discussion

After polymerization, the latexes were stable and transparent. However, due to the larger particle size of the particles and the higher refractive index of the poly(MADQUAT) compared with the monomer, the latexes dispersed more light than the initial microemulsions. Calorimetric measurements were used to estimate the heat of the reaction of MADQUAT at 20°C: $Q_r = 56$ kJ/mol.

3.1. Batch polymerizations

Fig. 1 presents the time evolution of the polymerization rate in runs 1 and 2. It can be seen that the process was initially very rapid, reaching a maximum value of R_p at about 10% conversion. Later the polymerization rate decreased until the process stopped. Both polymerizations stopped at the same time. Fig. 2 presents the evolution of the monomer conversion in these experiments. It can be seen that a limiting conversion (which increased with the initiator concentration) was reached in both cases. Table 1 presents the values of the particle diameters and number of polymer particles of the latexes obtained in the batch experiments. It can be seen that d_p decreased and N_p increased when the initiator concentration increased.

The fact that both polymerizations reached limiting conversions suggests that the initiator was very reactive and disappeared rapidly. Once the initiator was consumed the polymerization stopped because the lifetime of the radicals is rather short [5]. In addition, the fact that both polymerizations stopped at the same time indicates that the initiator disappeared according to a first order kinetics, i.e. the conversion of the initiator, x_I, was independent of the

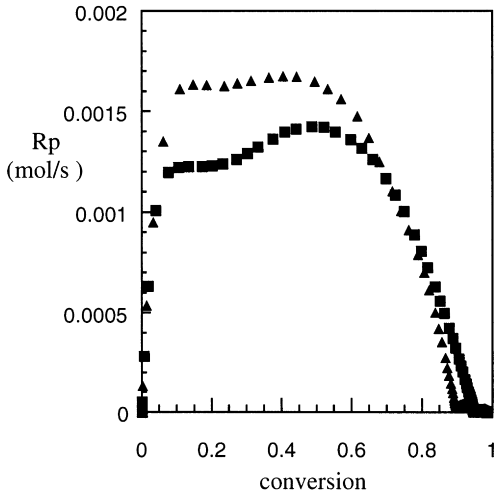

Fig. 3. Effect of the initiator concentration on the polymerization rate in the semi-continuous experiments: (▲) run 3; (■) run 4.

initial concentration of the initiator

$$x_I = 1 - \exp(-k_I t) \quad (5)$$

where k_I is the rate constant for the reaction between the metabisulfite and the monomer.

This result is in agreement with the reaction scheme given in Eq. (1) when there is an excess of monomer.

Fig. 2 shows that the polymerization rate increased with the initiator concentration. The maximum value showed a 0.47 order dependence upon the initiator concentration. Although this result was obtained with only two points, it coincided with the dependency of R_p upon [AIBN] observed in the photo-initiated inverse microemulsion polymerization of MADQUAT [5]. This value is not easy to interpret in a dispersed system because the reaction rate depends on both the number of polymer particles (N_p) and the average number of radicals in the particles ($\bar{n}$), both of which are

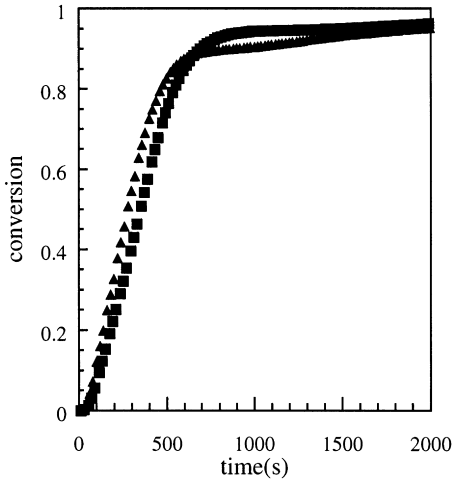

Fig. 4. Effect of the initiator concentration on the time evolution of the monomer conversion in the semi-continuous experiments: (▲) run 3; (■) run 4.

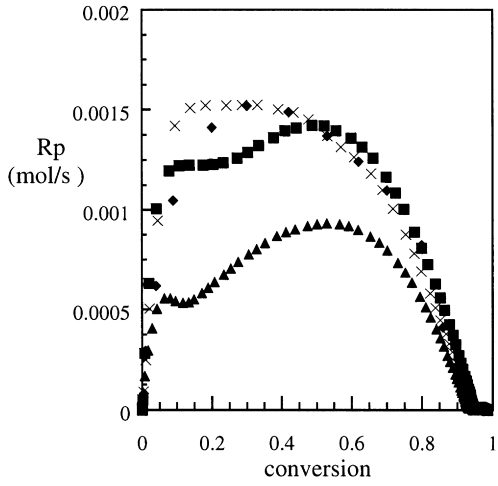

Fig. 5. Evolution of R_p in runs 4–7: (■) run 4; (×) run 5; (◆) run 6; and (▲) run 7.

affected by the initiator concentration and are interrelated. Also, it has to be taken into account that in this case active radicals are formed one by one in the disperse phase, while in the reactions of Ref. [5] radicals are formed in pairs in the continuous phase. The role of $CH_3–C^{\cdot}XCH_3$ radicals and the continuous phase in the termination reactions remains a matter of speculation.

3.2. Semi-continuous polymerizations

Fig. 3 presents the evolution of the polymerization rate in runs 3 and 4 in which the initiator concentration in the feed (0.00319 and 0.00182 g/cm^3, respectively) was varied (keeping the feed rate of the initiator solution constant at 2 g/min for 60 min). The values of the particle size and the number of polymer particles are presented in Table 2. Several intervals can be distinguished in the process (Fig. 3). First, R_p increased rapidly, then remained constant

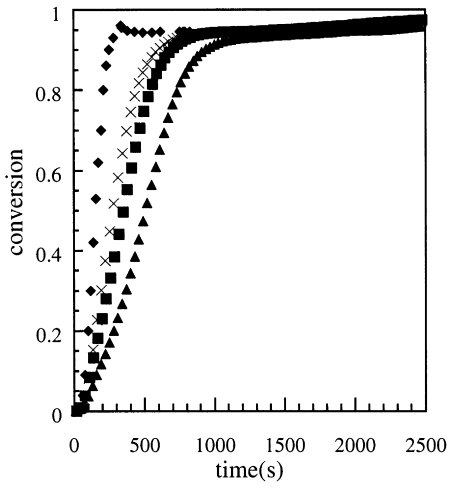

Fig. 6. Evolution of monomer conversion in runs 4–7: (■) run 4; (×) run 5; (◆) run 6; and (▲) run 7.

Table 3
Results obtained varying the weight fractions of aqueous phase, emulsifier and cyclohexane in the semi-continuous polymerizations at $T = 20°$ C (fractions are referred to the total amount of microemulsion)

Run	Weight fraction of aqueous phase	Weight fraction of emulsifier	Weight fraction of cyclohexane	d_p (nm)	N_p (particles)	R_{pmax} (mol/s)	$\bar{n}/\bar{n}_4$	$(\bar{n}/V_p)/(\bar{n}/V_p)_4$
4	0.34	0.13	0.53	116	3.1×10^{17}	1.4×10^{-3}	1	1
5	0.28	0.13	0.59	111	3.0×10^{17}	1.53×10^{-3}	1.05	1.26
6	0.15	0.13	0.72	90	2.9×10^{17}	1.52×10^{-3}	1.136	2.43
7	0.28	0.11	0.61	121	2.3×10^{17}	9.38×10^{-4}	0.88	0.77

for some time, later increased again, and finally decreased to zero. The shape of the plots in Fig. 3 are similar to those in Fig. 1 (batch process) where the second increase of R_p appeared as a shoulder in the decreasing part of the R_p evolution. The mechanisms that may yield this kind of evolution are discussed below. The evolution of monomer conversion in these experiments is shown in Fig. 4. It can be seen that high conversions were reached in short periods of time when the initiator was continuously fed during the process. This is an additional support of the idea that the limiting conversions obtained in the batch runs were due to the complete consumption of the initiator.

Varying amounts of aqueous phase, emulsifier and cyclohexane were used in runs 4–7. The amount of initiator was kept constant in these experiments. Figs. 5 and 6 show the evolution of polymerization rate and monomer conversion, respectively, in those experiments. It has to be pointed out that different amounts of monomer were used. Considering the reactions in which the same amount of emulsifier was used (runs 4–6), it can be seen in Fig. 5 that the evolution of run 5 is intermediate between that of run 4 where two peaks can be observed and run 6 that presents a single peak.

Table 3 shows that the particle diameter increases with the (aqueous phase/emulsifier) ratio. For the batch inverse microemulsion of MADQUAT, photo-initiated by UV light in the presence of AIBN, Sáenz de Buruaga et al. [5] reported that the diameter of the polymer particles was proportional to (aqueous phase volume/emulsifier volume)$^{2/3}$. This relationship can be justified by a model in which the nucleation occurred by the entry of radicals into the micelles and assuming that the entry occurred by a diffusional mechanism (the entry rate coefficient being proportional to the radius of the micelle). Fig. 7 shows that this relationship was also valid for the runs carried out in the semi-continuous reactor using sodium metabisulfite as initiator. It is surprising that the same relationship is valid in such different systems: radicals produced in the continuous phase and batch reactor (Sáenz de Buruaga et al. [5]), and radicals produced in the disperse phase and semi-continuous reactor (Fig. 7). The main difference between those systems was the locus in which the radicals were produced. The type of reactor was less important in the sense that its main effect was on the initiator concentration, as the rest of components were initially charged into the reactor.

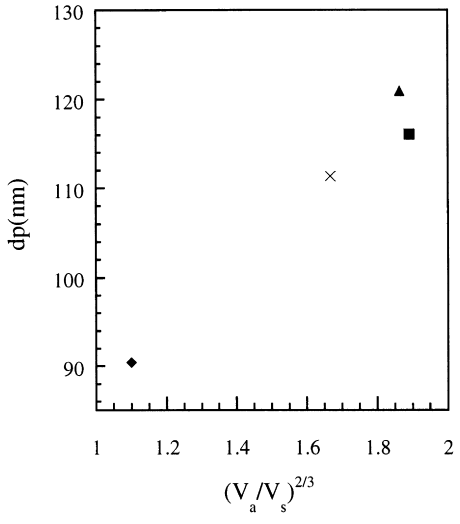

Fig. 7. Effect of (aqueous phase volume/emulsifier volume)$^{2/3}$ $(V_a/V_s)^{2/3}$ on the particle size: (■) run 4; (×) run 5; (◆) run 6; and (▲) run 7.

The rate of nucleation of micelles containing the initiator can be estimated if the rate of generation of radicals and their activity are known [15], but unfortunately none of these parameters are known in the present case. Nevertheless, the calculations performed by Alduncin et al. [16] on the nucleation rate of monomer droplets containing solubilized initiator, for the miniemulsion polymerization of styrene, may help to understand the present system. Alduncin et al. [16] used the balance of radicals in the monomer droplets and assumed that droplets were nucleated when a chain of 200 monomeric units was formed inside them. They found that, for droplets between 10 and 100 nm, the nucleation rate was almost proportional to the droplet size. Although the present system differs from that considered by Alduncin et al. [16], it is likely that the rate of nucleation per swollen micelle also increased with the micelle size with a power close to one. This will make nucleation similar to the case reported by Sáenz de Buruaga et al. [5] and this will yield the same d_p vs. (aqueous phase volume/emulsifier volume)$^{2/3}$ relationship.

Fig. 7 and Table 3 show that run 7 presented a behavior different from the other reactions. In particular, the particle diameter is bigger than that expected for its (aqueous phase volume/emulsifier volume) ratio. A similar case was reported by Sáenz de Buruaga et al. [5] for polymerizations

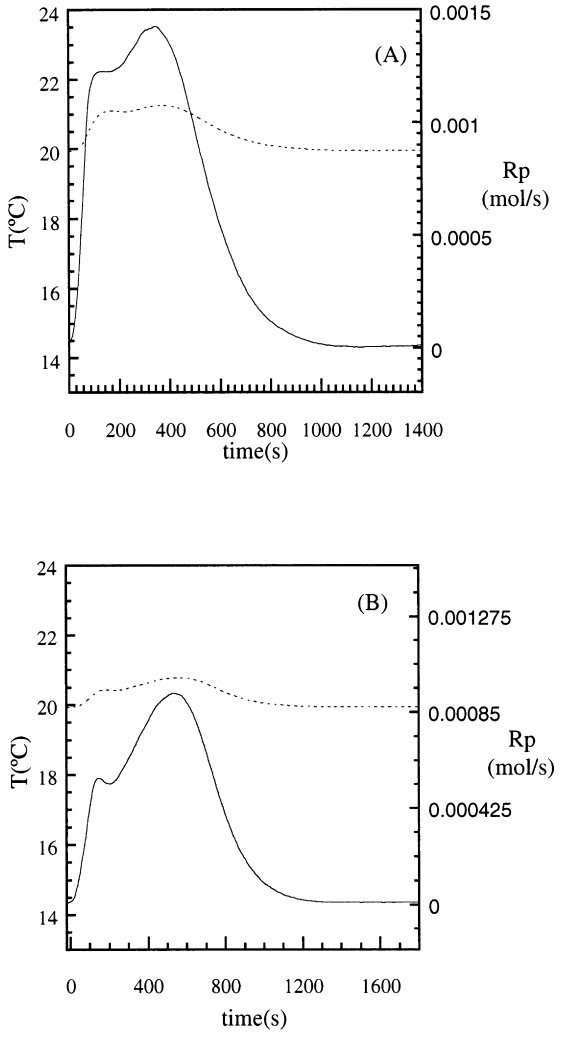

Fig. 8. Evolutions of reactor temperature (- - -) and polymerization rate (—) in: (A) run 4; (B) run 7.

with a high (aqueous phase volume/emulsifier volume) ratio, suggesting that limited coagulation might be the reason for the large particle size.

Table 3 presents the values of $\bar{n}$ and the concentration of radicals in the polymer particles normalized with respect to the values of these variables in run 4. Normalized values were used because the value of the propagation rate was unknown. The normalized values were calculated as follows:

$$\frac{\bar{n}_{\mathrm{run}i}}{\bar{n}_{\mathrm{run4}}} = \frac{R_{\mathrm{p}_{\mathrm{run}i}}[M]_{\mathrm{p}_{\mathrm{run4}}} N_{\mathrm{p}_{\mathrm{run4}}}}{R_{\mathrm{p}_{\mathrm{run4}}}[M]_{\mathrm{p}_{\mathrm{run}i}} N_{\mathrm{p}_{\mathrm{run}i}}} \tag{6}$$

where the values of the polymerization rates (R_p) and the number of polymer particles (N_p) are given in Table 3 and the monomer concentrations ($[M]_p$) were calculated from the partitioning equations [14].

It can be seen that $\bar{n}_6 > \bar{n}_5 > \bar{n}_4 > \bar{n}_7$. These differences are even more acute in terms of the concentration of radicals in the polymer particles. This suggests that this order also applies to the rate of generation of radicals in the polymer particles. Following this reasoning, the order of initiator concentrations should be $[\mathrm{initiator}]_6 > [\mathrm{initiator}]_5 > [\mathrm{initiator}]_4 > [\mathrm{initiator}]_7$. However, this is not the order that would be obtained if all the metabisulfite were dissolved in the aqueous phase ($[\mathrm{initiator}]_6 > [\mathrm{initiator}]_7 = [\mathrm{initiator}]_5 > [\mathrm{initiator}]_4$). A possible explanation for these results is that the transport of the metabisulfite is affected by diffusional limitations. The controlling step would be either the mass transfer between the droplets of the initiator solution entering the reactor and the continuous medium (transport by diffusion) or the coagulation rate between the droplets of the initiator solution and micelles and polymer particles (transport by coagulation). In both cases, the mass transfer rate would increase if the droplets of the initiator solution were smaller, namely, if the entering initiator solution were efficiently emulsified. Table 3 shows that for runs 4–6 the availability of the emulsifier (emulsifier/aqueous phase ratio) presents the same order than the concentration of radicals in the polymer particles. This seems to indicate that the transport of metabisulfite from the droplets of the initiator solution to the particles was accelerated by the availability of the emulsifier.

3.3. Polymerization rate evolution

An aspect that remains to be discussed is the shape of the polymerization rate plots. It is worth pointing out that the detection of these shapes has been possible because the calorimeter reactor measures directly the heat generation rate, which is proportional to the polymerization rate. The measure of a cumulative magnitude (such as monomer conversion) will mask the details of the R_p evolution. Thus, Fig. 1 cannot be obtained from Fig. 2. The calorimetric reactor used in this work does not have a cryostat, and hence it is not easy to control the reactor temperature at 20°C, in particular for rapid polymerizations. Actually, a slight increase of the reactor temperature was observed in most of the reactions. In order to check if the shape of the R_p plots was the result of variations of temperature in the reactor, a comparison between the evolution of these variables was carried out. Fig. 8 presents this comparison for runs 4 and 7. It can be seen that the second peak in the R_p plots is not due to a poor control of the reactor temperature, but it is an intrinsic characteristic of the process.

The shape of the R_p plots is similar to that found by Özdeger et al. [17–19] in the conventional emulsion polymerization of butyl acrylate stabilized with a non-ionic emulsifier. The measure of R_p was also carried out with a calorimetric reactor. According to Özdeger et al. [17–19] the first increase of R_p was due to the primary nucleation of polymer particles. As part of the emulsifier was solubilized in the monomer droplets, the particles did not find the emulsifier to stabilize their growth and coagulated leading to a decrease of R_p. When the monomer droplets disappeared, the emulsifier was released and a secondary nucleation

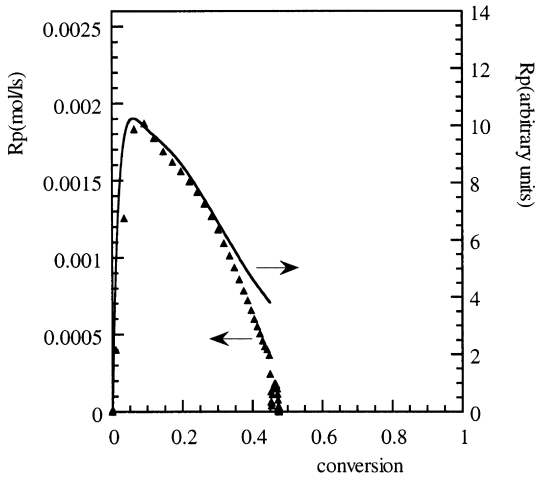

Fig. 9. Evolution of the experimental and predicted polymerization rates in the batch operation: (▲) run 2; (—) predicted $R_p = [I][M]N_p$ (from Eqs. (7)–(9)).

occurred yielding a new increase of the polymerization rate. Non-ionic emulsifiers that could be dissolved in the organic phase were also used in the present work. However, the volume of the cyclohexane remained almost constant during the whole process and it is hard to imagine a process that allows the release of the emulsifier at intermediate stages of the process.

A possible explanation of the shape of the R_p plots is as follows: In the batch operation, the process started when the aqueous solution of $Na_2S_2O_5$ was injected into the reactor containing the inverse microemulsion of MADQUAT. The metabisulfite was transported to the micelles where it reacted with the monomer initiating the polymerization (following the reaction scheme of Eq. (1)). This resulted in a rapid increment of the polymerization rate. However, the high R_p could not be maintained because of: (i) the decrease of the concentration of the monomer in the polymer particles due to the rapid consumption by polymerization and the relatively slow mass transfer from the micelles, and (ii) the consumption of the initiator. In contrast, the number of particles increased due to the continuous nucleation. This process was responsible for the shoulder that appeared on the evolution of R_p. However, the initiator was consumed rapidly and the polymerization stopped well before complete conversion. This qualitative explanation can be somehow assessed by using an admittedly crude model for these processes. Let us consider the following evolutions of the concentration of the monomer in the polymer particles, $[M]$, initiator concentration, $[I]$, and number of polymer particles, N_p (all of them in arbitrary units).

$$[M] = 2 + 6\exp(-27x), \tag{7}$$

$$[I] = 8\exp(-6x), \tag{8}$$

$$N_p = 10x - 7x^2 + 5x^3 \tag{9}$$

where x is the monomer conversion. Eq. (7) accounts for the decrease of the concentration of the monomer in the polymer particles from the initial value to a value in which the rate of consumption by polymerization is equal to the rate of mass transfer from the polymer particles. Eq. (8) accounts for the consumption of the initiator. Eq. (9) represents the increase of the number of polymer particles observed by Sáenz de Buruaga et al. [6] in the inverse microemulsion polymerization of MADQUAT initiated by UV in the presence of AIBN. It has to be pointed out that although the initiation system was different than that used in the present work, it has been shown above that there are many similarities in the way nucleation occurred in both systems.

It is reasonable to assume that the polymerization rate is proportional to $[I][M]N_p$. Fig. 9 compares the evolution of R_p predicted by this equation (in arbitrary units) with that of run 2. It can be seen that the shape of these plots is very similar. Obviously, this similarity cannot be taken as an unambiguous proof of the mechanisms proposed, but it shows that these mechanisms are plausible.

In the semi-continuous process, the first initiator fed into the reactor nucleated polymer particles that reacted rapidly because the concentration of the monomer in the swollen micelles was initially high. This caused the first increase of the polymerization rate. Later, the polymerization rate per particle decreased because of the decrease of the monomer and initiator concentrations. This decrease was due to the relatively rapid polymerization (and initiation) as compared with the mass transfer. As the polymerization rate per particle decreased and the number of polymer particles increased, a region in which R_p may decrease, stay constant or even increase might result depending on the relative rates of these processes. The decrease of the concentrations of monomer and initiator were likely to be limited as, at some point, the rates of polymerization and mass transfer would be roughly equal, and hence the values of the concentrations of the monomer and the initiator in the particles would be approximately constant (it is worth mentioning that the increase in the number of polymer particles may result in continuously decreasing concentrations, but this decrease would be slow as compared with the initial decrease). When the concentrations of monomer and initiator in the particles were constant, the polymerization rate increased again as N_p increased continuously. Finally, R_p decreased due to the monomer consumption.

As for the case of the batch process it is possible to develop a simplistic model that accounts for these mechanisms:

$$[M] = 2 + 6\exp(-27x) \qquad \text{for } x < 0.45, \tag{10}$$

$$[M] = (2 + 6\exp(-27x))(1 - (x - 0.45)/0.55) \qquad \text{for } x > 0.45, \tag{11}$$

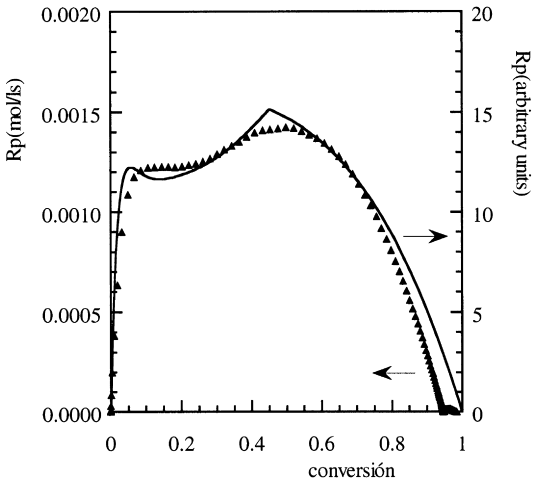

Fig. 10. Evolution of the experimental and predicted polymerization rates in the semi-continuous operation: (▲) run 4; (—) predicted $R_p = [I][M]N_p$ (from Eqs. (10)–(13)).

$$[I] = 2 + 8\exp(-9x), \tag{12}$$

$$N_p = 10x - 7x^2 + 5x^3. \tag{13}$$

Eq. (10) accounts for the initial decrease of the monomer concentration in the polymer particles until a constant value was reached. Eq. (11) accounts for the decrease of [*M*] in the final part of the process. Eq. (12) describes the initial decrease of [*I*] until a constant value was reached (the initiator was continuously fed into the reactor), and Eq. (13) accounts for the continuous nucleation. Fig. 10 compares the evolution of the simulated R_p (assuming it is proportional to $[I][M]N_p$) with that of run 4. As in the case of the batch process, this cannot be claimed to be a proof of the mechanisms outlined above, but it shows that these mechanisms are reasonable.

4. Conclusions

The kinetics of the inverse microemulsion polymerization of MADQUAT initiated with sodium metabisulfite in both batch and semi-continuous reactors were studied. It was found that the metabisulfite was able to initiate the polymerization at low temperature (20°C).

It was found that in the batch reactor the polymerization stopped well before the complete conversion of the monomer. The limiting conversion increased with the initiator concentration and was due to the complete consumption of the initiator, which disappeared according to first order kinetics. This was in agreement with the initiation mechanism proposed by Mukherjee et al. [7]. The polymerization rate was proportional to $[I]^{0.4-0.5}$, suggesting a bimolecular termination (it has to be pointed out that this result is based on only two points).

High conversions were reached in short periods of time when the initiator was continuously fed during the process. This additionally supported the idea that the limiting conversions obtained in the batch runs were due to the complete consumption of the initiator. It was found that the particle size depended on the two-third power of the (aqueous phase volume/emulsifier volume) ratio. This was the same relationship found by Sáenz de Buruaga et al. [5] for the batch inverse microemulsion polymerization of MADQUAT initiated by UV light in the presence of AIBN. The reason for the similarity seems to be the linear dependence of both nucleation processes on the size of the micelles. In the semi-continuous process, the transport of the metabisulfite from the droplets of the initiator solution to the particles seemed to be diffusionally limited and was accelerated by the availability of the emulsifier. The polymerization rate showed a complex evolution during the process that seemed to be the result of the interplay between transport phenomena, polymerization and initiation rates, and nucleation rate.

Acknowledgements

The financial support from the Diputación Foral de Gipuzkoa, the CICYT (grant 00TAP95-1020) and the Basque Government (project PGV 9209) is gratefully appreciated. A. Sáenz de Buruaga acknowledges a fellowship from the Ministerio Español de Educación y Ciencia.

References

[1] Candau F. In: Asua JM, editor. Polymeric dispersions: principles and applications. Dordrecht: Kluwer Academic, 1997.
[2] American Cyanamid Co. European Patent Appl, 0374457, 1989.
[3] Institut Francais du Petrole, French Patent Appl, 2565623, 1984.
[4] American Cyanamid Co., European Patent Appl, 0374478, 1989.
[5] Sáenz de Buruaga A, de la Cal JC, Asua JM. J Polym Sci, Part A: Polym Chem 1998;36:737.
[6] Sáenz de Buruaga A. PhD dissertation. Universidad del País Vasco, San Sebastián, Spain, 1998.
[7] Mukherjee R, Ghosh P, Chadhe SC, Palit SR. Makromol Chem 1964;80:208.
[8] Kim K, Griffith JR. J Colloid Interface Sci 1976;55:191.
[9] Candau F, Leong YS, Fitch R. J Polym Sci: Polym Chem Ed 1985;23:193.
[10] Burns DT, Townshend A, Carter AH. Inorganic reaction chemistry. Volume 2: Reactions of the elements and their compounds. Chichester: Ellis Horwood, 1981.
[11] Gugliotta LM, Arotçarena M, Leiza JR, Asua JM. Polymer 1995;36:2019.
[12] Gugliotta LM, Leiza JR, Arotçarena M, Armitage PD, Asua JM. Ind Engng Chem Res 1995;34:3899.
[13] Sáenz de Buruaga I, Armitage PD, Leiza JR, Asua JM. Ind Engng Chem Res 1997;36:4243.
[14] Sáenz de Buruaga A, de la Cal JC, Asua JM. J Polym Sci, Part A: Polym Chem 1999;12: in press.
[15] Smith WV, Ewart RH. J Chem Phys 1948;16:592.
[16] Alduncin JA, Forcada J, Asua JM. Macromolecules 1994;27:2256.
[17] Ozdeger E, Sudol ED, El-Aasser MS, Klein A. J Polym Sci, Part A: Polym Chem 1997;35:3813.
[18] Özdeger E, Sudol ED, El-Aasser MS, Klein A. J Polym Sci, Part A: Polym Chem 1997;35:3827.
[19] Özdeger E, Sudol ED, El-Aasser MS, Klein A. J Polym Sci, Part A: Polym Chem 1997;35:3837.